Title

Using spatial tracking with magnetic resonance imaging/ultrasound-guided biopsy to identify unilateral prostate cancer

Journal

BJU International, 125(3)

ISSN

1464-4096

Authors

Zhou, Steve R
Priester, Alan M
Jayadevan, Rajiv
et al.

Publication Date

2020-03-01

DOI

10.1111/bju.14943

HHS Public Access

Author manuscript

BJU Int. Author manuscript; available in PMC 2020 August 24.

Published in final edited form as:

BJU Int. 2020 March ; 125(3): 399–406. doi:10.1111/bju.14943.

Using Spatial Tracking with MRI/Ultrasound-Guided Biopsy to Identify Unilateral Prostate Cancer

Steve R. Zhou[a], **Alan M. Priester, PhD**[b,c], **Rajiv Jayadevan, MD**[b], **David C. Johnson, MD, MPH**[d], **Jason J. Yang**[a], **Jorge Ballon**[a], **Shyam Natarajan, PhD**[b,c], **Leonard S. Marks, MD**[b]

[a]David Geffen School of Medicine, University of California, Los Angeles

[b]Department of Urology, University of California, Los Angeles

[c]Department of Bioengineering, University of California, Los Angeles

[d]Department of Urology, University of North Carolina, Chapel Hill

INTRODUCTION

Hemi-gland ablation (HGA) of the prostate is an evolving treatment option for patients with unilateral clinically significant prostate cancer (csCaP). In contrast with traditional whole-gland interventions, HGA leaves intact the contralateral neurovascular bundle and other critical anatomical structures, thus increasing the patient's chance for preserving sexual and urinary function. HGA using both cryotherapy and high-intensity focused ultrasound have demonstrated excellent side effect profiles and very low complication rates, with promising intermediate-term cancer control[1–6]. Pending the delivery of long-term mortality data, this can be an attractive alternative that preserves quality of life for appropriately selected patients[7,8].

Proper selection of patients with csCaP located exclusively in a single lobe is the key to maximizing the efficacy of focal therapies like HGA[7,8]. We previously demonstrated that contemporary diagnostic tools—multiparametric MRI (mpMRI) with combined targeted and systematic biopsy under image guidance—fail to detect significant contralateral lesions and midline extension in between 40–48% of potential candidates for HGA[9,10]. Other studies have since confirmed this finding[11], and identification of prostate cancer (CaP) laterality for HGA continues to be a challenge.

Targeted biopsy with MRI/ultrasound (MRI/US) fusion devices allows for the spatial tracking of biopsy core locations that, when correlated with imaging and pathology data, can provide more precise tumor localization than the general sextant. Spatial relationships such as the distance between a positive core and the prostate midline are intuitively predictive of midline tumor extension. Classification and Regression Tree (CART) analysis is an intuitive

Corresponding Author: Steve R. Zhou, 681 East Meadow Drive, Palo Alto, CA 94306, Phone (650) 796-1026, Fax (310) 794-0987, szhou@mednet.ucla.edu.

Disclosures

Dr. Marks and Dr. Natarajan are co-founders of Avenda Health, Inc.

Dr. Alan Priester consults for Avenda Health, Inc.

and validated way to build decision trees for guiding clinical decision-making[12,13], with successful applications for predicting heart failure mortality and cancers with unknown primaries[14,15]. We sought to improve csCaP laterality prediction by applying CART analysis to spatially tracked fusion biopsy data.

SUBJECTS AND METHODS

Study Population and Experimental Design

For this IRB-approved study, we identified patients at a single institution who underwent combined systematic and targeted biopsy under MRI/US guidance and subsequently received radical prostatectomy (RP) between May 2011 and August 2018. All patients provided informed consent. We excluded patients for whom biopsy coordinates or MRI targets were unextractable from the fusion device or otherwise unavailable, as well as patients who received RP more than one year after the most recent usable biopsy. We also excluded patients who previously received any form of prostate focal therapy, or exhibited extra-prostatic disease on MRI.

Two independent sets of predictions for csCaP laterality were produced for this study population based on biopsy and imaging results: a “naïve” prediction (i.e. laterality based on biopsy and MRI reports alone, blinded to tracked location), and one using tracked biopsy and imaging data to derive a decision tree (DT) model. Corresponding whole mount prostatectomy (WMP) specimens were used as ground truth to verify concordance of the laterality decision made in each set of predictions (Figure 1).

Multi-Parametric MRI and MRI/US-Guided Biopsy

All patients received 3-Tesla mpMRI according to a standardized protocol with pelvic external phased array coils, with or without endorectal coil, either with the Siemens Magnetom Trio, Skyra or Verio (Siemens Medical Systems, Malvern, Pennsylvania, USA). MpMRIs were interpreted using PI-RADSv2[16] by a single abdominal imaging fellow and confirmed by one of three attending abdominal radiologists with 600, 2000, and 3000 prior prostate mpMRI reads. Cases prior to 2015 were interpreted using a previously described system similar to, but predating, the development of PI-RADSv2[17].

All biopsies were performed by a single urologist (LSM) using the Artemis system (Eigen, Grass Valley, CA), and included an average of 12 systematic cores combined with an average of 5 targeted cores taken from any suspicious PI-RADSv2 lesions (Grade ≥ 3).

Whole-Mount Processing of Prostatectomy Specimens

Following radical prostatectomy, each WMP specimen was sectioned from base to apex in 4–5mm intervals in the axial plane. Sections were mounted on slides and read by two fellowship-trained genitourinary pathologists, with four and twelve years of experience. A genitourinary radiologist and pathologist reviewed each case at a monthly tumor board to confirm reads on all lesions. All radiographic and pathologic features of each lesion were entered prospectively into a research database, and linked to biopsy information extracted from the fusion system (Figure 2).

Definitions of Unilateral csCaP

Ground truth unilateral csCaP was defined as unilateral Gleason Grade Group (GG) 2–4 on WMP specimens: a patient must have 1) presence of lesion(s) >GG1, 2) no bilateral or midline extension of lesions >GG1, for which HGA would leave residual cancer, and 3) no lesion >GG4, for which HGA would be deemed undertreatment due to metastatic risk[7,18]. Presence of any Gleason pattern 5 disease was also an exclusion criterion. Contralateral or bilateral GG1 lesions were not considered exclusion criteria. HGA was assumed to treat ipsilateral capsular involvement.

"Naïve" unilateral csCaP was defined as apparent unilateral GG2–4 demonstrated by mpMRI with combined systematic and targeted biopsy of PI-RADSv2 lesions grade ≥3. No biopsy-confirmed lesion with csCaP could exhibit midline extension on mpMRI. If there were multiple biopsy-confirmed MRI lesions, they must have all been unilateral. Combined systematic and targeted biopsy must have demonstrated presence of unilateral GG2–4 disease, and no core could contain >GG4 disease or any pattern 5 disease. Contralateral and bilateral GG1 was allowed.

For the DT model, a patient was deemed to have unilateral csCaP if the model predicted higher than a 50% chance for unilateral GG2–4 disease on WMP based on biopsy- and image-based features.

Data Extraction and Feature Generation

We used two prospectively-maintained databases: one that linked fusion biopsy to pathology and MRI results, and another that described lesion features on WMP. Custom Matlab 2018b (MathWorks, Natick, MA) scripts were written to extract and compute all data features, also known as covariates when using standard multivariable analysis terminology. All imaging and pathology reports in patient charts were checked manually by four separate authors (SRZ, DCJ, JJY, JB) to ensure accuracy of the extracted data.

In addition to obtaining standard clinicopathologic features used in routine diagnosis and assessment—age, PSA-related features, prostate volume, biopsy results, mpMRI results, etc.—biopsy coordinates were used to compute various spatial features that were likely predictive of bilateral or midline extension of csCaP (Figure 3). Examples include but are not limited to: distance between prostate midline and nearest positive biopsy core, distance between midline and the nearest suspicious PI-RADSv2 lesion, and the presence of a negative biopsy core between a biopsy-confirmed lesion and midline. All features involving distance measures were scaled to a 40cc prostate, approximated as a sphere. A full list of features considered can be found in Supplemental Table 1.

Developing the Decision Tree

All model design was performed with custom Python code using open-source packages from Scikit-learn[19]. Specifically, our custom python code employed the "tree.DecisionTreeClassifier" package for CART analysis. Model inputs included all features mentioned above. Model output was the probability of unilateral csCaP on WMP.

To limit over-fitting and to retain interpretability, we limited the DT model to a maximum tree depth of two, resulting in a maximum of three possible branch points[12,13].

Performance Assessment and Statistical Analysis

The DT model was evaluated with the area under the curve (AUC) statistic derived from the receiver operator characteristic (ROC) curve[20]. Comparative metrics were accuracy, sensitivity, and positive predictive value. Accuracy and sensitivity were compared to naïve laterality predictions using the McNemar test. Positive predictive value was compared with the Chi squared test.

RESULTS

Model Design and Performance

229 patients met initial inclusion criteria. One patient was excluded for not having a recent biopsy. Three were excluded for having had focal therapy. 52 patients did not have coordinates available from biopsy. In total, 173 patients were eligible for analysis. The resulting decision tree is depicted in Figure 4. Our model showed that, if a CaP-positive biopsy or biopsy-confirmed MRI lesion was close to midline (within one third of the prostate radius), contralateral csCaP was likely present. For this CART-selected feature, the distance was taken to the closest cancer-containing object, which was either 1) a positive core, including GG1, or 2) the nearest edge of a biopsy-confirmed MRI lesion.

Concordance Rates with Ground Truth Laterality

Of 173 patients, 50 had unilateral csCaP on WMP (30%). Overall, laterality decisions based on biopsy and MRI reports alone were concordant with WMP in 127/173 (73%) of cases. The DT model improved concordance to 80%, although this improvement was not statistically significant (p=0.13). AUC was 0.82 (Figure 5).

66 cases appeared to have unilateral csCaP based on naïve biopsy and mpMRI, of which 31 (47%) were incorrect. 25/66 (38%) of these cases were due to undetected contralateral disease, defined as either midline extension of tumor, missed distinct contralateral tumor, or both on WMP. The DT model identified 19 cases of unilateral csCaP, of which only 4 cases were incorrect (3 due to undetected contralateral disease). By adding a minimum cutoff for the distance between midline and detected cancer, the DT model decreased the error rate from 47% to 17% (p=0.01). This cut-off equates to 1/3 of the distance between midline and the lateral border of the gland for any size of prostate. This improvement came at a cost to sensitivity: naïve biopsy and mpMRI found 35/50 (70%) of cases that were unilateral on WMP, while the DT model only detected 19 (38%, p<0.01). All metrics are summarized in Table 1.

Reasons for Discordance

Naïve laterality predictions were discordant with WMP in 46 cases. All reasons for discordance of naïve predictions are summarized in Table 2.

41 (89%) appeared to be unilateral csCaP on biopsy and MRI, but were not on WMP. The most common cause for discordance was missed midline extension of the dominant lesion, occurring in 19 (41%) cases. There was a distinct undetected contralateral csCaP lesion in 11 (24%) cases, five of which also had midline extension of the dominant lesion. Of these 25 cases of undetected contralateral csCaP, 13 (52%) had positive cores from the contralateral side with GG1. Additionally, six (13%) cases were due to upgrading of biopsy-derived GG on WMP. Three (7%) cases had ipsilateral csCaP downgraded to GG1 disease in the dominant tumor on WMP.

Biopsy and MRI incorrectly identified 15 (33%) of the discordant cases as ineligible for HGA. In 5 cases, a pathologically unilateral lesion was over-contoured on MRI such that it appeared to cross midline. Another 5 cases were upgraded from unilateral GG1 on biopsy to unilateral GG2–4 on WMP. 4 cases were downgraded from GG5 on biopsy to unilateral GG2–4 on WMP. 1 case had bilateral csCaP on biopsy with only unilateral csCaP on WMP.

DISCUSSION

In this analysis of 173 patients, we confirmed that contemporary diagnostics are insufficient for identifying unilateral csCaP: use of biopsy and MRI reports alone in this cohort would have resulted in incomplete ablation in 25 of 66 patients (38%) due to undetected contralateral csCaP. We addressed this need by using CART analysis to derive a single additional criterion to improve positive predictive value; by filtering out patients with cancer detected near midline, only three of 19 (16%) selected patients harbored undetected contralateral csCaP. We also included all additional risk-stratification metrics that have been reported in the literature in our analysis (PSA, prostate volume, PSAD, age, etc.), only to find that no other metric was as predictive of focal unilateral disease as biopsy-derived spatial features in a decision tree model (Supplemental Table 1). Excluding patients with tumor located near midline substantially decreases the likelihood of missing contralateral cancer in potential HGA candidates (increased specificity). However, this comes as the expense of incorrectly excluding HGA candidates from this treatment modality (decreased sensitivity). We must weigh the risk of inadequate oncologic control and exposure to an unnecessary and ineffective treatment against the potential benefits of maximizing the HGA eligibility pool.

CART analysis was employed over a multivariate model in order to deliver the most clinically straightforward message. Nonetheless, we performed an exploratory univariate and multivariate analysis, the results of which are listed in Supplemental Table 1. The results confirm the strongest predictors of unilateral disease to be covariates that express either bilaterality of cancer or proximity of detected cancer to midline. Other risk-stratification covariates such as age, PSA, and PSAD were not significant predictors of disease laterality.

Our baseline prediction results—blinded to tracked biopsy and target locations—are consistent with existing literature. We previously reported a 48% rate of undetected contralateral disease in a cohort of 92 patients with apparent unilateral csCaP based on MRI/US-guided biopsy[10]. In a larger similar study of 185 patients, Choi and colleagues found contralateral CaP on WMP in 67.5% of patients exhibiting apparent unilateral cancer

≤GG2 based on MRI/US-guided biopsy[11]. Previous analyses based on conventional trans-rectal ultrasound (TRUS) biopsy report similar rates of discordance[21,22].

The underlying challenge at hand is reliable identification of tumor margins, for which the limitations of modern diagnostics have been well-demonstrated. While the PI-RADSv2 system has shown good sensitivity for detecting the presence csCaP lesions[16], much of the pathologic tumor extends beyond the borders of the contoured MRI lesion: in a 2017 study correlating MRI lesions to final pathology for 222 tumors, Priester and colleagues reported that the underlying tumor was on average 11mm longer in diameter and three times greater in volume than the T2-weighted MRI lesion segmentation[23]. Based on this observation, on average, a biopsy-confirmed lesion 5 to 7mm from midline would harbor cancer that comes within a millimeter of crossing over. This distance is approximately equal to one third of the distance from midline to the lateral edge of a 40cc prostate, the cutoff criteria proposed in the present study.

For the purposes of focal therapy, underestimation of true tumor extent is a critical shortcoming that decreases treatment efficacy. Studies with mandated whole-gland biopsy at 1 year following HGA report between 10 and 20% cancer detection rate contralateral to the treated half of the prostate[24,25]. The rates of contralateral disease undetected on biopsy in these studies is also likely significant based on emerging analyses, which can lead to subsequent insidious progression to higher-risk disease[9–11]. Despite the recognition of these diagnostic limitations, no reported consensus paper for identifying focal therapy candidates incorporates selection criteria that account for MRI-invisible tumor extension[7,18]. The present study is unique in that it uses tracked biopsy and target coordinates to interrogate the exact locations of csCaP detected during diagnosis, and correlate these spatial metrics to the risk for midline extension.

Reliable margin detection is not the only challenge in selecting patients for HGA. Discordance between biopsy- and WMP-determined GG is common even with MRI/US-guided biopsy[26], and contributed to incorrect laterality predictions in 18 of 46 cases (39%). Because pathologic grade discordance is beyond the scope of the present study, we minimized its impact by expanding our selection criteria to encompass the widest tolerable range of pathologic grade based on our review of consensus guidelines, conceding that including patients with GG4 is not a universally accepted practice[7,18]. However, it is important to consider biopsy grading accuracy when offering focal therapies like HGA.

Due to sampling limitations, it is intuitive that proportions of Gleason patterns in a biopsy core correlate poorly with those found in the entire underlying tumor. Targeted cores sampling the central focus can over-represent the highest pattern disease. A GG2 or GG3 tumor might exhibit midline extension with a region of only GG1 disease, presenting as clinically insignificant contralateral GG1 on biopsy. Perhaps for this reason, studies have shown that the concordance of Gleason grading between biopsy and RP can be improved by 1) increasing the density of biopsy cores[27] or 2) increasing the accuracy through targeted biopsy[26,28]. This observation can explain why filtering out patients with *any* cancer detected near midline is more effective than looking only at cores and targets bearing csCaP. Incomplete ablation that leaves exclusively low-risk residual regions of the dominant tumor

has unknown clinical significance. However, based on the index lesion theory, residual cells from the dominant focus still arise from the same progenitor, which may drive tumor growth and harbor metastatic potential regardless of pathologic grade[29,30]. Furthermore, prior work indicates that up to 27% of patients with GG1 will progress to GG2 or higher on repeat biopsy within a year[31].

Our study is not without limitations. Low sample size and an unbalanced dataset limit the study's power. Additionally, due to the lack of validation either with an external dataset or internal cross-validation, the conclusions of this study are at best exploratory; further analysis with more patients would help establish external validity of the proposed DT model. Our study also has an element of selection bias for two reasons. First, because all patients ultimately received RP, they are likely a higher risk cohort than the standard focal therapy population. Second, because a significant portion of patients were referred for MRI/US-guided biopsy due to prior negative TRUS biopsies, this population likely harbors tumors frequently undetected by standard 12-core sampling. Third, a comprehensive analysis of focal therapy would analyze a wider range of ablation schema beyond HGA only. For example, many patients with focal anterior midline lesions could feasibly undergo anterior quadrant ablations. However, the limited sample size of the study at hand prohibited more detailed analysis. Finally, we recognize that no clear consensus exists for selecting the appropriate candidate for focal therapies such as HGA at this time; some institutions exclude patients with GG4 and treat patients with large-volume GG1, while others deem all contralateral GG1 and even micro-residual ≥GG2 disease to be clinically-insignificant; some institutions employ additional PSA or PSAD cut-offs, while others are beginning to incorporate genetic testing to supplement patient selection[7,18]. More long-term outcomes data are needed to establish exactly the correct population for focal therapy.

In conclusion, solely relying on biopsy and MRI reports may lead to undetected contralateral prostate cancer for which HGA is insufficient. However, conservatively selecting patients with tumors limited to the lateral two-thirds of the prostate appears to drastically improve the ability of HGA to fully encapsulate the index lesion.

Supplementary Material

Refer to Web version on PubMed Central for supplementary material.

Acknowledgments

Supported in part by Award R01CA158627 from the National Cancer Institute. The content is solely the responsibility of the authors and does not necessarily represent the official views of the National Cancer Institute or the National Institutes of Health. Other support by the UCLA Dean's Leadership in Health and Sciences Scholarship, the UCLA Clinical and Translational Sciences Institute Grant No. UL1TR000124, the Jean Perkins Foundation, the Kent Kresa family foundation, and the Steven C. Gordon Family Foundation.

REFERENCES

1. Guillaumier S, Peters M, Arya M, et al. A Multicentre Study of 5-year Outcomes Following Focal Therapy in Treating Clinically Significant Nonmetastatic Prostate Cancer. Eur Urol 2018;74(4):422–429. doi:10.1016/j.eururo.2018.06.006 [PubMed: 29960750]

2. Valerio M, Ahmed HU, Emberton M, et al. The role of focal therapy in the management of localised prostate cancer: A systematic review. Eur Urol 2014;66(4):732–751. doi:10.1016/j.eururo.2013.05.048 [PubMed: 23769825]
3. Golan R, Bernstein AN, McClure TD, et al. Partial Gland Treatment of Prostate Cancer Using High-Intensity Focused Ultrasound in the Primary and Salvage Settings: A Systematic Review. J Urol 2017;198(5):1000–1009. doi:10.1016/j.juro.2017.03.137 [PubMed: 28433640]
4. Barqawi AB, Huebner E, Krughoff K, O'Donnell CI. Prospective Outcome Analysis of the Safety and Efficacy of Partial and Complete Cryoablation in Organ-confined Prostate Cancer. Urology. 2018;112:126–131. doi:10.1016/j.urology.2017.10.029 [PubMed: 29126844]
5. Zhou SR, Simopoulos DN, Jayadevan R, et al. Use of MRI-Guided Biopsy for Selection and Follow-up of Men Undergoing Hemi-gland Cryoablation of Prostate Cancer. Urology. 2019;126:158–164. doi:10.1016/j.urology.2018.11.052 [PubMed: 30659903]
6. Ward JF, Jones JS. Focal cryotherapy for localized prostate cancer: A report from the national Cryo On-Line Database (COLD) Registry. BJU Int 2012;109(11):1648–1654. doi:10.1111/j.1464-410X.2011.10578.x [PubMed: 22035200]
7. Jarow JP, Ahmed HU, Choyke PL, Taneja SS, Scardino PT. Partial gland ablation for prostate cancer: Report of a food and drug administration, American urological association, and society of urologic oncology public workshop. Urology. 2016;88:8–13. doi:10.1016/j.urology.2015.11.018 [PubMed: 26621480]
8. Spillman D FDA Oncology Center of Excellence Public Workshop: Development of Treatments for Localized Prostate Cancer. US Food and Drug Administration https://www.fda.gov/NewsEvents/MeetingsConferencesWorkshops/ucm608328.htm.
9. Nassiri N, Chang E, Lieu P, et al. Focal Therapy Eligibility Determined by Magnetic Resonance Imaging/Ultrasound Fusion Biopsy. J Urol 2018;199(2):453–458. doi:10.1016/j.juro.2017.08.085 [PubMed: 28830754]
10. Johnson DC, Yang JJ, Kwan L, et al. Do contemporary imaging and biopsy techniques reliably identify unilateral prostate cancer? Implications for hemiablation patient selection. Cancer. 2019;125(17):2955–2964. doi:10.1002/cncr.32170 [PubMed: 31042322]
11. Choi YH, Yu JW, Kang MY, et al. Combination of multiparametric magnetic resonance imaging and transrectal ultrasound-guided prostate biopsies is not enough for identifying patients eligible for hemiablative focal therapy for prostate cancer. World J Urol 2019;(0123456789). doi:10.1007/s00345-018-02617-2
12. Lewis RJ. An introduction to classification and regression tree (CART) analysis. 2000 Annu Meet Soc Acad Emerg Med San Fr Calif 2000 http://ci.nii.ac.jp/naid/10010792827/en/. Accessed March 20, 2019.
13. Lavanya D, Rani KU. Performance Evaluation of Decision Tree Classifiers on Medical Datasets. Int J Comput Appl 2011;26(4):1–4. doi:10.5120/3095-4247
14. Fonarow GC, Adams KF, Abraham WT, Yancy CW, Boscardin WJ. Risk stratification for in-hospital mortality in acutely decompensated heart failure: Classification and regression tree analysis. J Am Med Assoc 2005;293(5):572–580. doi:10.1001/jama.293.5.572
15. Hess KR, Abbruzzese MC, Lenzi R, Raber MN, Abbruzzese JL. Classification and regression tree analysis of 1000 consecutive patients with unknown primary carcinoma. Clin Cancer Res 1999;5(11):3403–3410. [PubMed: 10589751]
16. Weinreb JC, Barentsz JO, Choyke PL, et al. PI-RADS Prostate Imaging – Reporting and Data System: 2015, Version 2. Eur Urol 2016;69(1):16–40. doi:10.1016/j.eururo.2015.08.052 [PubMed: 26427566]
17. Natarajan S, Marks LS, Margolis DJA, et al. Clinical application of a 3D ultrasound-guided prostate biopsy system. Urol Oncol Semin Orig Investig 2011;29(3):334–342. doi:10.1016/j.urolonc.2011.02.014
18. Tay KJ, Scheltema MJ, Ahmed HU, et al. Patient selection for prostate focal therapy in the era of active surveillance: An International Delphi Consensus Project. Prostate Cancer Prostatic Dis 2017;20(3):294–299. doi:10.1038/pcan.2017.8 [PubMed: 28349978]
19. Pedregosa F, Varoquaux G, Gramfort A, et al. Scikit-learn: Machine Learning in Python. J Mach Learn Res 2012;12:2825–2830. doi:10.1007/s13398-014-0173-7.2

20. Hanley JA, McNeil BJ. The meaning and use of the area under a receiver operating characteristic (ROC) curve. Radiology. 1982;143(1):29–36. doi:10.1148/radiology.143.1.7063747 [PubMed: 7063747]
21. Fumadó L, Cecchini L, Juanpere N, Ubré A, Lorente JA, Alcaraz A. Twelve Core Template Prostate Biopsy is an Unreliable Tool to Select Patients Eligible for Focal Therapy. Urol Int 2015;95(2):197–202. doi:10.1159/000381559 [PubMed: 25896142]
22. Jung J-W, Lee BK, Choi WS, et al. Combination of clinical characteristics and transrectal ultrasound-guided biopsy to predict lobes without significant cancer: application in patient selection for hemiablative focal therapy. Prostate Int 2014;2(1):37–42. doi:10.12954/PI.13031 [PubMed: 24693533]
23. Priester A, Natarajan S, Khoshnoodi P, et al. Magnetic Resonance Imaging Underestimation of Prostate Cancer Geometry: Use of Patient Specific Molds to Correlate Images with Whole Mount Pathology. J Urol 2017;197(2):320–326. doi:10.1016/j.juro.2016.07.084 [PubMed: 27484386]
24. Feijoo ERC, Sivaraman A, Barret E, et al. Focal High-intensity Focused Ultrasound Targeted Hemiablation for Unilateral Prostate Cancer: A Prospective Evaluation of Oncologic and Functional Outcomes. Eur Urol 2016;69(2):214–220. doi:10.1016/j.eururo.2015.06.018 [PubMed: 26164416]
25. Rischmann P, Gelet A, Riche B, et al. Focal High Intensity Focused Ultrasound of Unilateral Localized Prostate Cancer: A Prospective Multicentric Hemiablation Study of 111 Patients. Eur Urol 2017;71(2):267–273. doi:10.1016/j.eururo.2016.09.039 [PubMed: 27720531]
26. Le JD, Stephenson S, Brugger M, et al. Magnetic resonance imaging-ultrasound fusion biopsy for prediction of final prostate pathology. J Urol 2014;192(5):1367–1373. doi:10.1016/j.juro.2014.04.094 [PubMed: 24793118]
27. San Francisco IF, DeWolf WC, Rosen S, Upton M, Olumi AF. Extended prostate needle biopsy improves concordance of gleason grading between prostate needle biopsy and radical prostatectomy. J Urol 2003;169(1):136–140. doi:10.1016/S0022-5347(05)64053-0 [PubMed: 12478121]
28. Borkowetz A, Platzek I, Toma M, et al. Direct comparison of multiparametric magnetic resonance imaging (MRI) results with final histopathology in patients with proven prostate cancer in MRI/ultrasonography-fusion biopsy. BJU Int 2016;118(2):213–220. doi:10.1111/bju.13461 [PubMed: 26935133]
29. Ahmed HU. The Index Lesion and the Origin of Prostate Cancer. N Engl J Med 2009;361(17):1704–1706. doi:10.1056/nejmcibr0905562 [PubMed: 19846858]
30. Liu W, Laitinen S, Khan S, et al. Copy number analysis indicates monoclonal origin of lethal metastatic prostate cancer. Nat Med 2009;15(5):559–565. doi:10.1038/nm.1944 [PubMed: 19363497]
31. Sonn GA, Chang E, Natarajan S, et al. Value of Targeted Prostate Biopsy Using Magnetic Resonance – Ultrasound Fusion in Men with Prior Negative Biopsy and Elevated Prostate-specific Antigen. Eur Urol 2014;65(4):809–815. doi:10.1016/j.eururo.2013.03.025 [PubMed: 23523537]

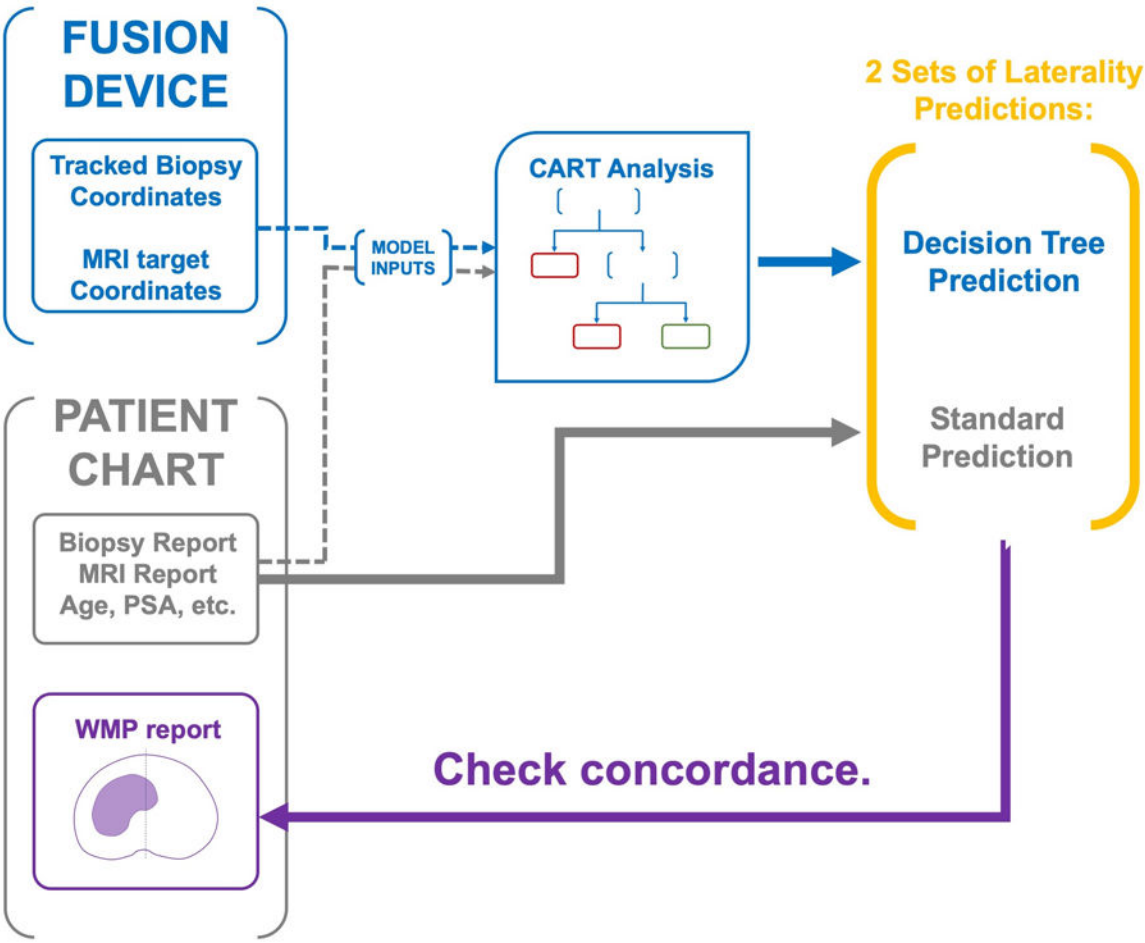

Figure 1.

Block diagram for experiment design. The typical diagnostic pathway for determining csCaP laterality is depicted in gray, which is based solely on biopsy- and MRI-proven laterality. Spatial data from the fusion device is combined with standard clinicopathologic parameters to create a decision tree model for predicting csCaP laterality (blue). Each prediction set's concordance with laterality on WMP is assessed (purple).

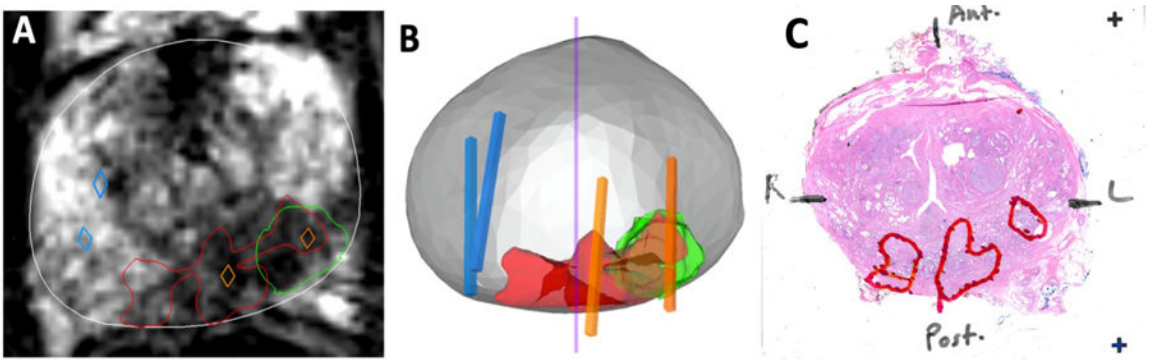

Figure 2.

Correlation of MRI (A), spatial biopsy pathology (B), and whole mount pathology (C). Suspicious MRI lesion (green in A and B) is shown to underestimate true tumor volume (red in A and B, outlined in C). Positive ipsilateral cores (orange) confirm intermediate disease in the MRI lesion and near midline. Negative contralateral cores in blue erroneously imply unilaterality of disease. Only a subset of tracked cores are shown for clarity.

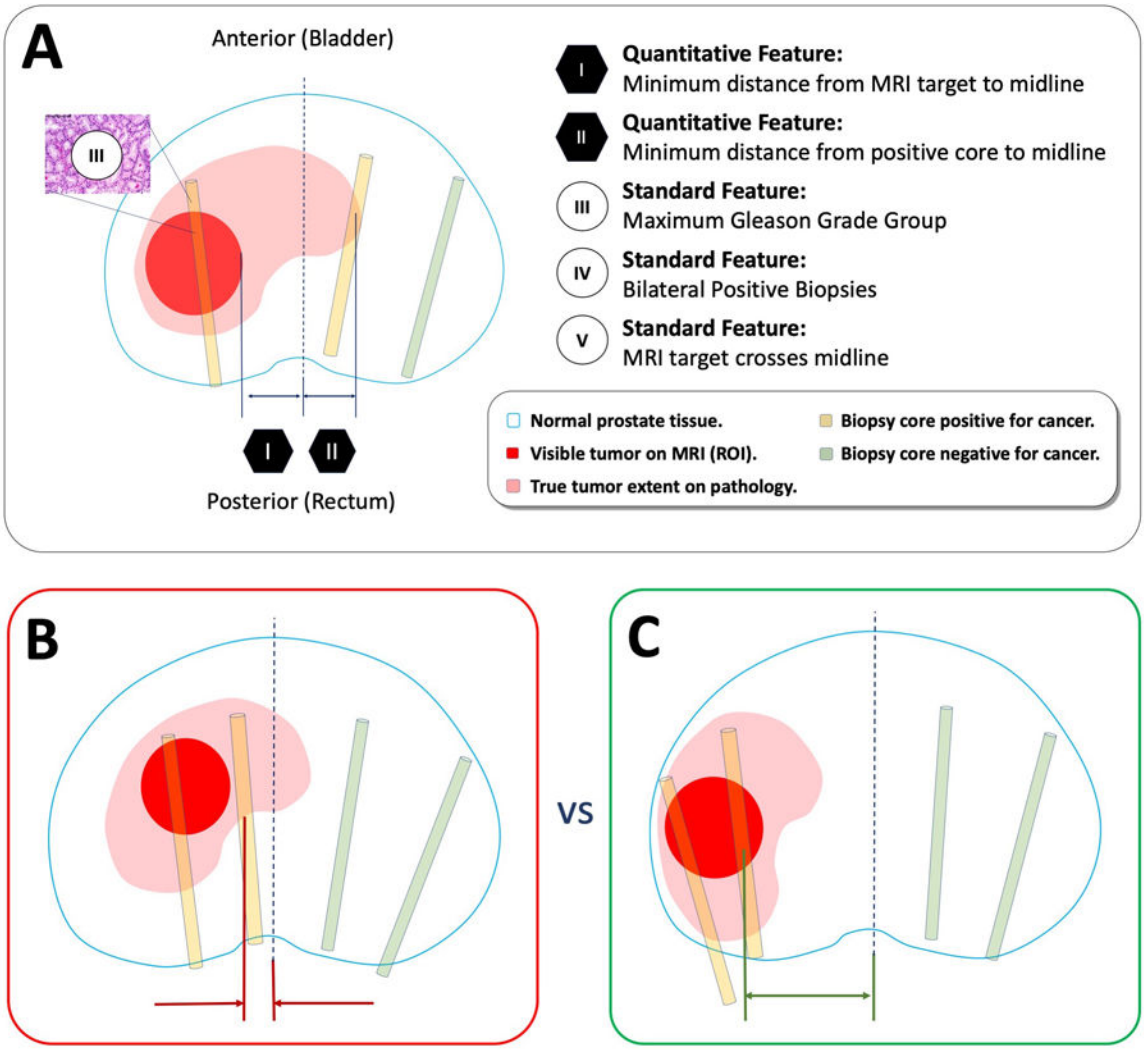

Figure 3.

A) Exemplary set of features predictive of unilateral GG2–4 CaP, annotated in an axial section diagram of the prostate. Shown are 2 features in relation to midline derived from spatial tracking, and 3 standard qualitative features derived from typical biopsy pathology reports. Spatial measurements like distance of nearest positive core to midline predict unilaterality of disease. Both 2B and 2C are unilateral by standard criteria, but a predictive model might flag case 2B over 2C due to close proximity of disease to midline.

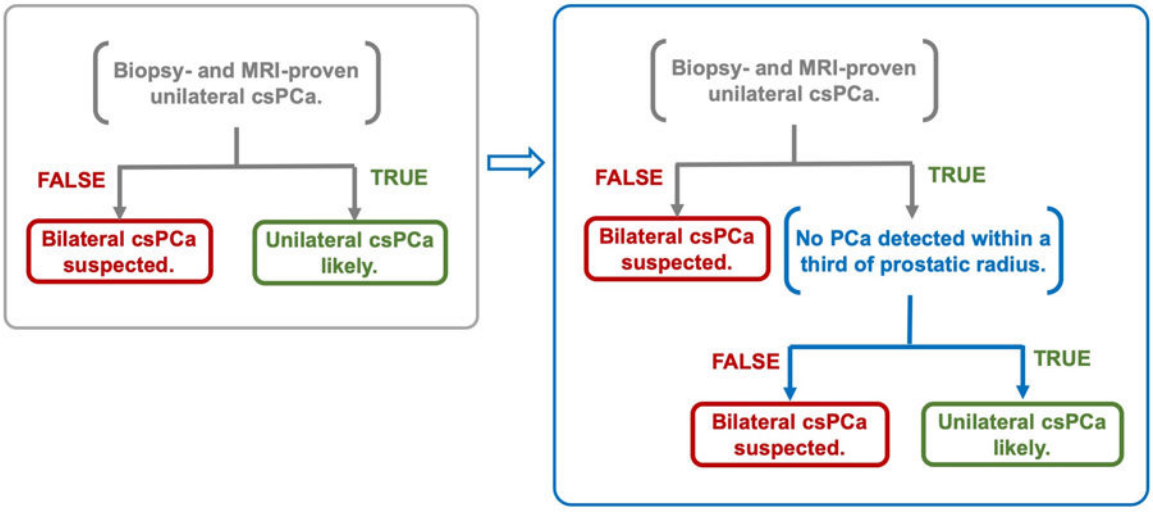

Figure 4.

LEFT: Decision tree representing current decision-making based on biopsy and mpMRI (naïve laterality prediction). RIGHT: Decision tree derived from CART analysis. Cases with biopsy- and MRI-proven unilaterality can be further filtered for missed midline extension by looking for cores within a third of the prostatic radius.

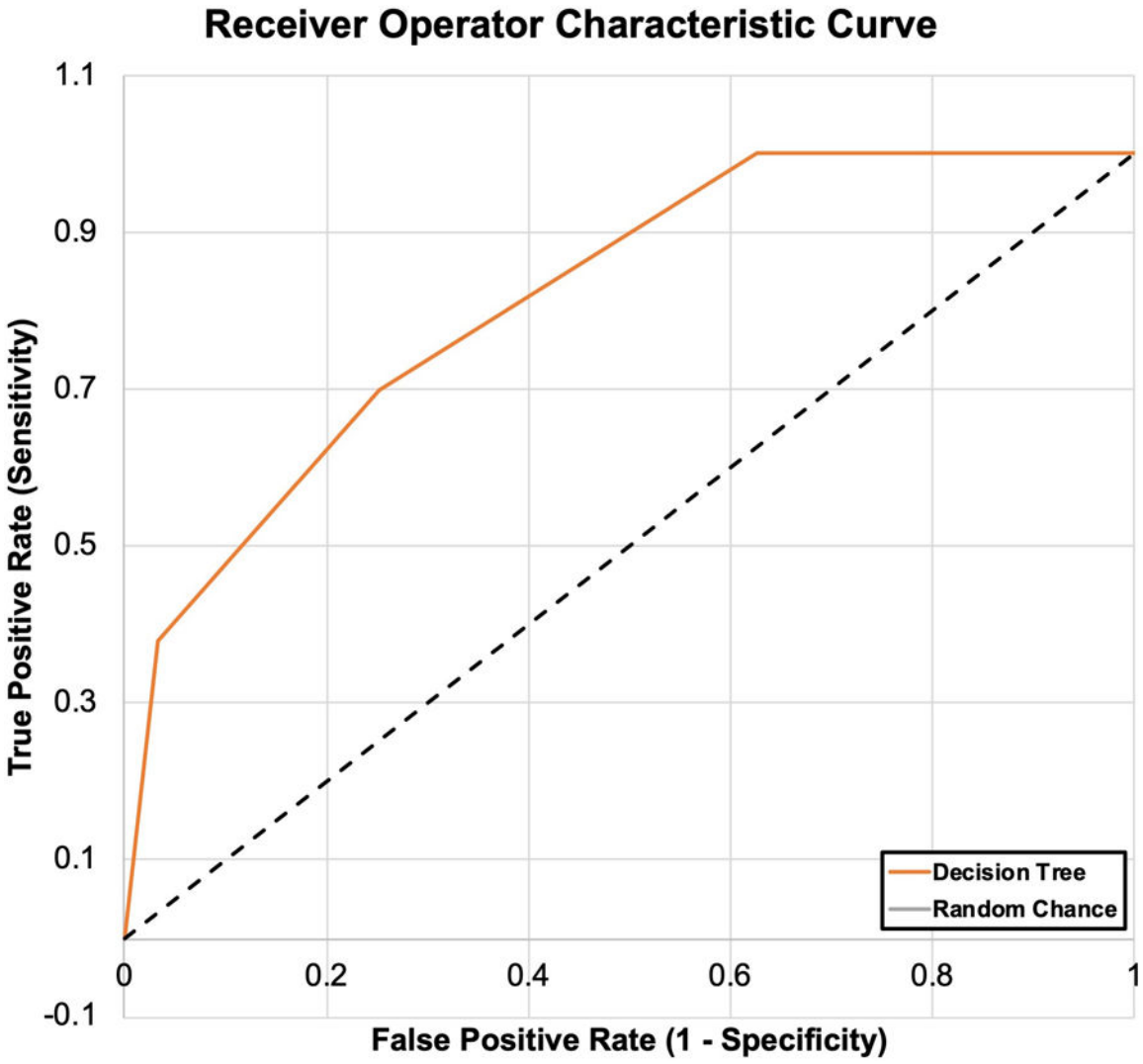

Figure 5.
ROC curve of DT model for identifying unilateral csCaP.

Table 1.

Summary statistics comparing performance between decision sets.

METRIC	NAÏVE PREDICTION	DECISION TREE
AUC	-	0.82
ACCURACY	0.73	0.80 (p=0.13)
SENSITIVITY	0.70	0.38 (p=0.0002)
PPV	0.53	0.83 (p=0.01)

Table 2.

Reasons for discordance of naïve laterality predictions with whole mount prostatectomy.

REASON FOR DISCORDANCE (TOTAL = 46)	N (%)
Bilateral csCaP on WMP (N = 31)	31 (67)
Undetected midline extension	19 (41)
Missed contralateral tumor	11 (24)
GG Upgraded on WMP	6 (13)
GG Downgraded on WMP	3 (7)
Unilateral csCaP on WMP (N = 15)	15 (33)
Over-contouring of MRI lesion	5 (11)
GG Upgraded on WMP	5 (11)
GG Downgraded on WMP	4 (9)
Under-sampling on WMP	1 (2)